

# Relation between Magnetic, Spectroscopic and Structural Properties of Binuclear Copper(II) Complexes of Pentadentate Schiff-base Ligand, Semi-empirical and ab-initio Calculations

Y. Elerman, H. Kara<sup>a</sup>, and A. Elmali

Department of Engineering Physics, Faculty of Engineering, Ankara University,  
06100 Besevler-Ankara, Turkey

<sup>a</sup> Department of Physics, Faculty of Art and Sciences, University of Balikesir,  
10100 Balikesir, Turkey

Reprint requests to Prof. Dr. A. E.; E-mail: elmali@eng.ankara.edu.tr

Z. Naturforsch. **58a**, 363 – 372 (2003); received January 7, 2003

The synthesis and characterization of  $[\text{Cu}_2(\text{L}^1)(3,5 \text{ prz})]$  ( $\text{L}^1 = 1,3\text{-Bis}(2\text{-hydroxy-3,5-chlorosalicylideneamino})\text{propan-2-ol}$ ) **1** and of  $[\text{Cu}_2(\text{L}^2)(3,5 \text{ prz})]$  ( $\text{L}^2 = 1,3\text{-Bis}(2\text{-hydroxy-bromosalicylideneamino})\text{propan-2-ol}$ ) **2** are reported. The compounds were studied by elemental analysis, infrared and electronic spectra. The structure of the  $\text{Cu}_2(\text{L}^1)(3,5 \text{ prz})$  complex was determined by x-ray diffraction. The magnetochemical characteristics of these compounds were determined by temperature-dependent magnetic susceptibility measurements, revealing their antiferromagnetic coupling. The superexchange coupling constants are  $210 \text{ cm}^{-1}$  for **1** and  $440 \text{ cm}^{-1}$  for **2**. The difference in the magnitude of the coupling constants was explained by the metal-ligand orbital overlaps and confirmed by ab-initio restricted Hartree-Fock (RHF) calculations. In order to determine the nature of the frontier orbitals, Extended Hückel Molecular Orbital (EHMO) calculations are also reported.

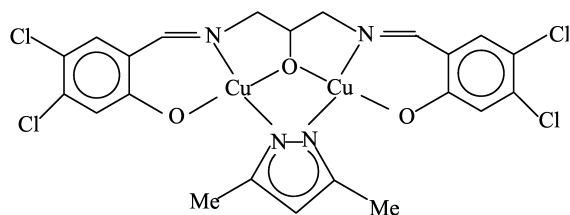
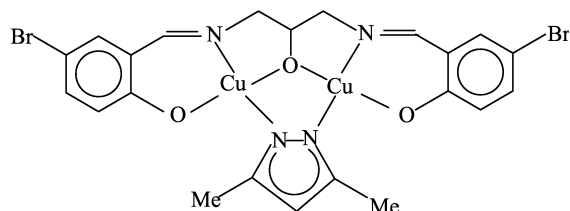
**Key words:** Dinuclear Copper(II) Complex; Antiferromagnetic Coupling; Overlap Interaction; Countercomplementary Effect; ab-initio Restricted Hartree-Fock Molecular Orbital Calculation.

## Introduction

Bridged binuclear complexes of first-row transition metals have received much attention recently because of their condensed-phase magnetic properties [1, 2]. Most extensively studied compounds are hydroxo-bridged Cu(II) binuclear complexes [3, 4]. These compounds are also of theoretical interest, because they provide examples of the simplest case of magnetic interactions with only two unpaired electrons. These Cu(II) complexes exhibit ferromagnetic or antiferromagnetic coupling depending on their geometry. Detailed analysis results in the linear correlation between the Cu-O-Cu angle and the singlet-triplet exchange parameter  $J$  established by Hodgson and coworkers [5], who proposed:  $J = -74.53\varphi + 7270 \text{ cm}^{-1}$  (in which  $\varphi$  is the Cu-O-Cu angle). Based on this correlation, an antiferromagnetic behaviour results for an angle larger than  $97.55^\circ$ , whereas smaller values produce a ferromagnetic coupling. Several theoretical calculations were performed to better understand this correlation [6, 7], and theoretical approaches were applied to un-

derstand the nature of the ferromagnetic / antiferromagnetic interaction [8].

To continue these investigations, the syntheses and characterization of  $[\text{Cu}_2(\text{L}^1)(3,5 \text{ prz})]$  ( $\text{L}^1 = 1,3\text{-Bis}(2\text{-hydroxy-3,5-chlorosalicylideneamino})\text{propan-2-ol}$ ) **1** of  $[\text{Cu}_2(\text{L}^2)(3,5 \text{ prz})]$  ( $\text{L}^2 = 1,3\text{-Bis}(2\text{-hydroxy-bromosalicylideneamino})\text{propan-2-ol}$ ) **2** are reported. The scheme of the molecules is given in Figs. 1 and 2. In a preceding study, we have described the preparation and magnetism of the dicopper(II) complexes  $[\text{Cu}_2(\text{L}^3)(3,5 \text{ prz})]$  ( $\text{L}^3 = 1,3\text{-bis}(2\text{-hydroxy-1-naphthylideneamino})\text{propan-2-ol}$ ) **3**,  $[\text{Cu}_2(\text{L}^4)(3,5 \text{ prz})]$ , ( $\text{L}^4 = 1,3\text{-bis}(2\text{-hydroxy-5-chlorosalicylideneamino})\text{propan-2-ol}$ ) **4** and  $[\text{Cu}_2(\text{L}^5)(3,5 \text{ prz})]$  ( $\text{L}^5 = 1,3\text{-bis}(2\text{-hydroxy-4-methoxybenzylidene amino})\text{propan-2-ol}$ ) **5** [9, 10, 11]. These compounds show antiferromagnetic behaviour ( $-2J$ :  $210 \text{ cm}^{-1}$  for **1**,  $440 \text{ cm}^{-1}$  for **2**,  $444 \text{ cm}^{-1}$  for **3**,  $164 \text{ cm}^{-1}$  for **4** and  $472 \text{ cm}^{-1}$  for **5**). In order to clarify these differences in the magnitude of the coupling constants, we carried out molecular orbital calculations of the 3,5-dimethylpyrazolate in **1** by ab-initio restricted Hartree-Fock (RHF)

Fig. 1. Structural diagram for the compound **1**.Fig. 2. Structural diagram for the compound **2**.

methods and compared our results with the literature. We also performed Extended Hückel Molecular Orbital (EHMO) calculations to determine the nature of the frontier orbitals.

## Experimental

### Preparation of Ligands

**Caution:** Perchlorate salts of metal complexes with organic ligands are potentially explosive. Even small amounts of material should be handled with caution.

The Schiff base ligands (**L**<sup>1</sup> and **L**<sup>2</sup>) were prepared by reaction of 1,3-diaminopropan-2-ol with 3,5-chlorosalicylaldehyde and 5-bromosalicylaldehyde (1:2 mol ratio) in methanol, respectively. The yellow Schiff bases precipitated from the solution on cooling.

### Preparation of Cu(II) Complexes

Complex **1** was obtained when a sample of the **L**<sup>1</sup> (1 mmol) in methanol (50 ml) was added dropwise to a stirred mixture containing 3,5-dimethylpyrazole (1 mmol) and copper(II) perchlorate hexahydrate (2 mmol) in methanol (25 ml). Triethylamine (3 mmol) was added to the solution. The mixture was stirred and thin green crystals were collected and washed with methanol. Recrystallization from acetone afforded single crystals suitable for x-ray structure determination. Complex **2** was prepared by similar procedures. (**1**: Found: C, 40.77; H, 2.98; N, 8.76%; C<sub>22</sub> H<sub>18</sub> N<sub>4</sub> O<sub>3</sub> Cl<sub>4</sub> Cu<sub>2</sub> Calcd: C, 40.32; H, 2.77; N, 8.55%; **2**: Found: C, 39.35; H, 3.19; N, 8.53%; C<sub>22</sub> H<sub>20</sub> N<sub>4</sub> O<sub>3</sub> Br<sub>2</sub> Cu<sub>2</sub> Calcd: C, 39.13; H, 2.99; N, 8.30%).

Table 1. Summary of crystallographic data for the compound **1**.

Empirical formula	C <sub>22</sub> H <sub>18</sub> Cu <sub>2</sub> Cl <sub>4</sub> N <sub>4</sub> O <sub>3</sub>
Formula weight (g.mol <sup>-1</sup> )	655.30
Crystal system	Triclinic
Space group	P $\bar{1}$
Unit cell dimensions	a [Å] = 8.074(1), b [Å] = 10.806(2), c [Å] = 13.605(2) $\alpha$ [°] = 91.93(3), $\beta$ [°] = 93.92(2), $\gamma$ [°] = 103.24(3)
V [Å <sup>3</sup> ]	1151.3 (2)
Z	2
D <sub>calc</sub> (g.cm <sup>-3</sup> )	1.89
$\mu$ [cm <sup>-1</sup> ]	23.5
Diffractometer	Enraf-nonius DIP2000
Radiation type	Mo-K $\alpha$ , $\lambda$ = 0.71073 Å
Temperature (K)	250
Index ranges	0 ≤ h ≤ 10, -13 ≤ k ≤ 13, -17 ≤ l ≤ 17
2 $\theta$ range for data collection	1.54 to 27
Reflections collected	4084
Independent reflections	2470
Refinement method	full-matrix, least-squares on F
Goodness-of-fit on F	1.015
Final R indices [I <sub>2</sub> σ(I)]	R = 0.071, wR = 0.056
Largest diff. peak, hole	0.36 and -0.87 e.Å <sup>-3</sup>

### Physical Measurements

Elemental (C, H, N) analyses were carried out by standard methods at the TUBITAK Research center (Ankara, Turkey). IR spectra were measured with a Perkin-Elmer Bx FT-IR instrument with the samples as KBr pellets in the 4000–400 cm<sup>-1</sup> range. Electronic spectra in acetone solutions in the 800–200 nm range were recorded on a Perkin-Elmer Lambda 2. Magnetic susceptibility measurements of the powdered sample were performed at 5–350 K with a MPMS Quantum Design SQUID magnetometer for **1** and a Faraday-type magnetometer for **2**. For details of the apparatus see [12, 13]. Diamagnetic corrections of the molar magnetic susceptibility of the compounds were applied, using Pascal's constants [14]. The applied field was 2 T for **1** and 1.2 T for **2**. The magnetic moments were obtained from the relation  $\mu_{\text{eff}} = 2.828(\chi T)^{1/2}$ .

### Crystal Structure Analysis

X-ray data collection was carried out on an Enraf-Nonius DIP2000 diffractometer [15] using a single crystal with the dimensions 0.2 × 0.3 × 0.3 mm with graphite monochromatized Mo-K $\alpha$  radiation ( $\lambda$  = 0.71069 Å) by an  $\omega$  scan technique. Data reduction was achieved using the DIP200 software, Denzo [15].

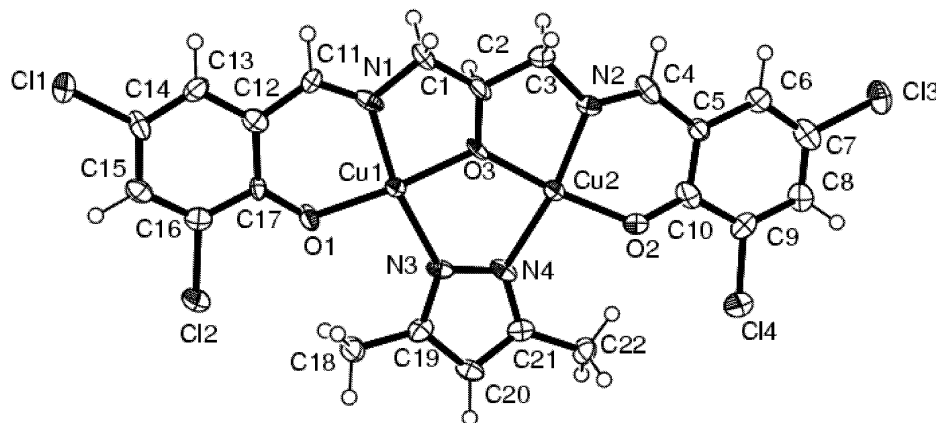


Fig. 3. Ortep Plot of the compound **1** (The numbering of the atoms corresponds to Table 2). Displacement ellipsoids are plotted at the 50% probability level and H atoms are presented as spheres of arbitrary radii.

Table 2. Atomic coordinates ( $\times 10^4$ ) and equivalent isotropic displacement parameters ( $\text{\AA}^2 \times 10^3$ ) for the compound **1**. Equivalent isotropic  $U(\text{eq})$  is defined as one third of the trace of the orthogonalized  $U_{ij}$  tensor.

Atom	x	y	z	$U(\text{eq})$
Cu1	1690(1)	677(1)	4024(1)	19
Cu2	2933(1)	-1006(1)	5893(1)	20
Cl1	250(4)	3070(2)	-806(2)	50
Cl2	-217(3)	4340(2)	2978(2)	35
Cl3	6172(3)	-5758(2)	8603(2)	44
Cl4	4219(3)	-1416(2)	9349(2)	44
O1	809(6)	1978(4)	3384(4)	26
O2	3643(7)	-1386(5)	7194(4)	31
O3	2447(7)	-731(5)	4548(4)	35
N1	1937(7)	-149(5)	2755(5)	25
N2	3646(7)	-2471(5)	5317(4)	20
N3	1981(7)	1386(5)	5407(5)	21
N4	2336(7)	667(5)	6186(5)	21
C1	2570(1)	-1296(7)	2886(7)	40
C2	2750(2)	-1551(1)	3882(7)	83
C3	3470(1)	-2589(7)	4227(6)	29
C4	4322(9)	-3269(6)	5795(6)	27
C5	4597(9)	-3299(6)	6834(5)	23
C6	5210(1)	-4346(6)	7192(6)	26
C7	5440(1)	-4451(7)	8173(7)	33
C8	5109(9)	-3567(6)	8840(6)	28
C9	4540(1)	-2547(7)	8493(6)	30
C10	4250(1)	-2324(6)	7469(7)	28
C11	1700(1)	250(7)	1882(5)	25
C12	1099(9)	1367(6)	1682(6)	24
C13	940(1)	1634(7)	675(6)	27
C14	412(9)	2710(6)	428(6)	27
C15	9(9)	3537(6)	1137(6)	27
C16	183(9)	3240(6)	2118(6)	25
C17	722(8)	2185(6)	2458(5)	18
C18	1520(1)	3586(7)	5187(6)	29
C19	1924(9)	2537(7)	5794(5)	25
C20	2242(9)	2582(6)	6809(6)	25
C21	2469(8)	1373(6)	7024(6)	22
C22	2860(1)	948(7)	8023(6)	29

Intensity data were corrected for Lorentz and Polarization effects. An empirical absorption correction was

Table 3. Selected bond lengths [ $\text{\AA}$ ] and angles [ $^\circ$ ] characterising the inner coordination sphere of the copper(II) centre for the compound **1** (see Fig. 3. for the adopted labelling scheme.)

Cu1 – Cu2	3.403(1)	Cu1 – O1	1.922(5)
Cu1 – O3	1.907(5)	Cu2 – O2	1.909(6)
Cu2 – O3	1.894(6)	Cu1 – N1	1.960(6)
Cu1 – N3	1.985(6)	Cu2 – N2	1.962(5)
Cu2 – N4	2.008(5)	N3 – N4	1.387(9)
Cu1 – O3 – Cu2	127.1(3)	O1 – Cu1 – O3	174.1(2)
O1 – Cu1 – N1	91.8(2)	O1 – Cu1 – N3	99.7(2)
O3 – Cu1 – N1	83.2(2)	O3 – Cu1 – N3	85.7(2)
N1 – Cu1 – N3	165.6(2)	O2 – Cu2 – O3	172.6(2)
O2 – Cu2 – N2	91.5(2)	O3 – Cu2 – N2	82.0(2)
O2 – Cu2 – N4	99.9(2)	O3 – Cu2 – N4	86.2(2)
N2 – Cu2 – N4	166.8(2)		

also performed by using DIFABS [16]. The structure was solved by SIR92 [17] and refined with CRYSTALS [18]. H atoms were refined using a riding model, and H atom displacement parameters were restricted to be  $1.2U_{\text{eq}}$  of the parent atom. A perspective drawing of the molecule is shown in Fig. 3 [19]. Table 1 summarizes the crystal data and data collection procedures for compound **1**. The final positional parameters are presented in Table 2. Selected bond lengths and angles are summarized in Table 3.

#### Molecular Orbital Calculations

The reported Ab-initio restricted Hartree-Fock (RHF) calculations for 3,5- dimethylpyrazolate were carried out by using the GAUSSIAN-98 program [20]. STO- 3G [21] minimal basis sets were adopted for carbon and nitrogen atoms. The molecular orbital calculations were performed using EHMO [22, 23] for the dinuclear complex, using the CACAO program [24]. The interatomic distances were taken from the X-ray re-

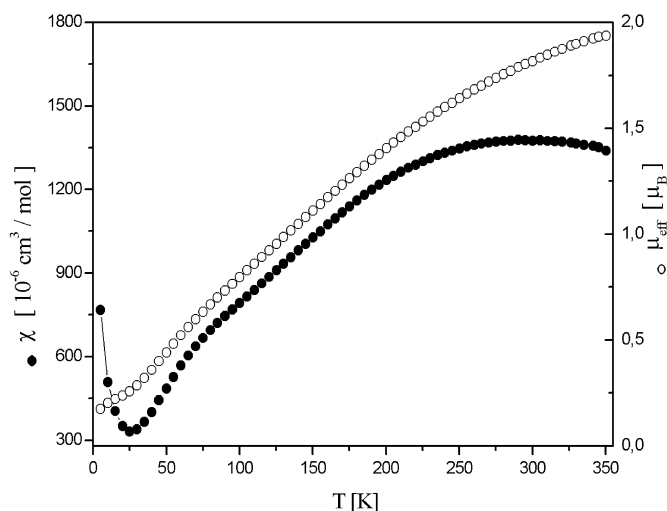


Fig. 4. Plots of molar susceptibility,  $\chi_M$ , and effective magnetic moment,  $\mu_{\text{eff}}$ , versus temperature for the compound **1**. The solid line represents the least squares fitting of the data.

Table 4. Spectral data for the compounds **1** and **2**.

	IR data ( $\text{cm}^{-1}$ )		Electronic data ( $\text{cm}^{-1}$ )	
	$\nu_{\text{as}}(\text{OH})$	$\nu_{\text{as}}(\text{C}=\text{N})$	Band I	Band II
<b>1</b>	3400	1630	16313	26109
<b>2</b>	3400	1600	18587	26109

sults. MO representations were plotted using CACAO software.

## Results and Discussion

### Spectroscopic Data

The IR spectra of both complexes show  $\nu(\text{OH})$  stretching vibrations of the hydroxo bridge at  $3400 \text{ cm}^{-1}$  (broad). The most characteristic band in the IR spectra corresponds to  $\nu(\text{C}=\text{N})$  stretching vibrations in the expected regions for the salicylideneamino compounds [25, 26]. This band occurs at  $1630 \text{ cm}^{-1}$  (sharp) for **1** and  $1600 \text{ cm}^{-1}$  (sharp) for **2**. The IR spectra of the complexes are similar.

The electronic spectra of both complexes show a broad absorption band (band I) in the visible region with a maximum at  $16313 \text{ cm}^{-1}$  (613 nm) for **1** and  $18587 \text{ cm}^{-1}$  (538 nm) for **2** (Table 4), which is assigned to a  $d \rightarrow d$  transition. This band is similar to corresponding pyrazolate-bridged dinuclear copper(II) complexes [27]. Moreover, the spectra of the complexes display a sharp band at  $26109 \text{ cm}^{-1}$  (383 nm) (band II), which is known to be characteristic for dinuclear copper(II) compounds with a square planar  $\text{Cu}_2\text{O}_2\text{N}_2$ -group and has been assigned to an  $\text{O} \rightarrow \text{Cu}$  charge transfer band [28, 29].

### Crystal Structure Description of the Compound **1**

The complex consists of binuclear molecules in which each copper ion is surrounded by two O and two N atoms in a square planar coordination. The Cu-N and Cu-O bond lengths are comparable with the bond lengths reported in other binuclear copper(II) complexes [30–33]. The distance between the two copper(II) centers is  $3.403(1) \text{ \AA}$  and the Cu-O-Cu bridging angle is  $127.1(3)^\circ$ , which is in the range of similar binuclear copper(II) complexes [34, 35]. The dihedral angle formed by the two coordination planes is  $170^\circ$ , and the whole molecule therefore is nearly planar. The sum of the bond angles around the bridging oxygen atom is  $359.9^\circ$ , indicating that the three bonds are essentially planar.

### Magnetism

Plots of the molar susceptibility and effective magnetic moment versus temperature for **1** and **2** are illustrated in Fig. 4 and Fig. 5, respectively. The observed magnetic susceptibility data were fitted to the modified Bleaney-Bowers equation [36],

$$\chi = \frac{Ng^2\mu_B^2}{3k(T-\Theta)} \left[ 1 + \frac{1}{3} \exp(-2J/kT) \right]^{-1} (1-x_p) \quad (1)$$

$$+ \frac{Ng^2\mu_B^2}{4kT} x_p + N\alpha,$$

using the isotropic Heisenberg–Dirac–Van Vleck Hamiltonian  $\mathbf{H} = -2JS_1 \cdot S_2$  for two interacting  $S = 1/2$  centers, where  $-2J$  is the energy difference

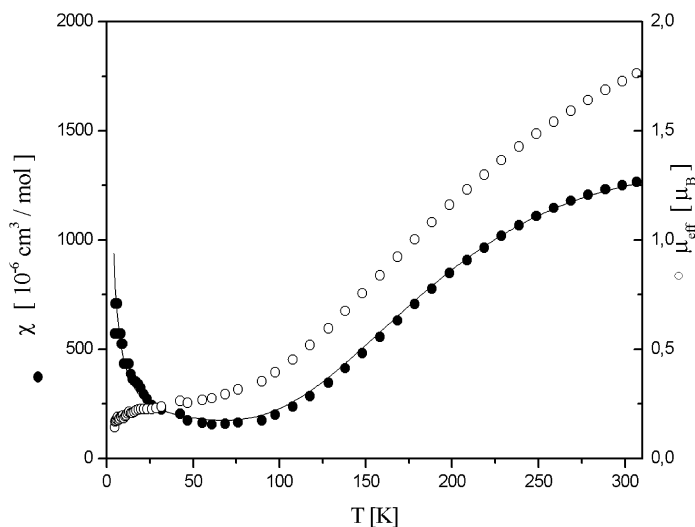


Fig. 5. Plots of molar susceptibility,  $\chi_M$ , and effective magnetic moment,  $\mu_{\text{eff}}$ , versus temperature the compound **2**. The solid line represents the least squares fitting of the data.

between spin-singlet and -triplet states.  $N_\alpha$  is the temperature-independent paramagnetism,  $x_p$  the fraction of a monomeric impurity, and  $\Theta$  is a Weiss-like correction for intermolecular interactions. Least squares fitting of the data leads to  $J = -210 \text{ cm}^{-1}$ ,  $g = 2.2$ ,  $x_p = 0.2\%$  and  $\Theta = -10 \text{ K}$  for **1**, and  $2J = -440 \text{ cm}^{-1}$ ,  $g = 2.2$ ,  $x_p = 0.3\%$  and  $\Theta = -11 \text{ K}$  for **2**. The non-zero value of  $\Theta$  may be due to the intermolecular interaction in the binuclear complex. In Figs. 4 and 5, the molar susceptibilities show a broad maximum at ca. 300 K for **1** and 270 K for **2**, indicative of an antiferromagnetically coupled system. A small amount of monomeric impurities in responsible for the increase in susceptibility below 15 K. The magnetic moments were obtained from the relation  $\mu_{\text{eff}} = 2.828(\chi T)^{1/2}$ . The observed and calculated  $\mu_{\text{eff}}$  decreases from  $1.76\mu_B$  at 300 K to  $0.16\mu_B$  at 5 K for **1** and from  $1.86\mu_B$  at 300 K to  $0.22\mu_B$  at 5 K for **2**. According to the empirical Hatfield-Hodgson correlation formula [5] one would expect the interaction to be as high as  $-2202.76 \text{ cm}^{-1}$ . The deviation from this formula can differ considerably due to additional structural effects.

#### Magnetostructural Correlations

Some interesting correlations between structural and magnetic parameters emerge from the data in Table 5. In general, binuclear copper(II) complexes have several structural features to affect the strength of exchange coupling interactions, such as the dihedral angle between the two coordination planes, the planarity

Table 5. Structural and magnetic data for a series of related compounds.

Compound	Cu...Cu [Å]	Cu-O-Cu [°]	(Cu-O) <sup>g</sup> [Å]	$\phi^h$ [°]	$\theta^i$	$-2J$ [cm <sup>-1</sup> ]
<b>1</b>	3.403(1)	127.1(3)	1.908(6)	170.0	359.9	210
<b>2</b>	—	—	—	—	—	440
<b>3</b>	3.365(1)	125.7(1)	1.901	165.0	359.0	440
<b>4</b>	3.368(1)	126.0(2)	1.894	178.6	355.6	472
<b>5</b>	3.355(1)	124.7(2)	1.898	166.8	355.3	164
<b>6</b>	3.359(4)	125.1(7)	1.897	176.2	359.9	240
<b>7</b>	3.349	121.7	1.894	172.6	343.0	310
<b>8</b>	3.360	121.8	1.916	164.2	359.6	540
<b>9</b>	3.377	125.9	1.895	178.1	—	550

<sup>1,2</sup> Present work; <sup>3</sup> [Cu<sub>2</sub>(L<sup>1</sup>)(3,5,prz)] (Kara et al. [10]); <sup>4</sup> [Cu<sub>2</sub>(L<sup>2</sup>)(3,5,prz)] (Kara et al. [9]); <sup>5</sup> [Cu<sub>2</sub>(L<sup>3</sup>)(3,5,prz)] (Kara et al. [11]); <sup>6</sup> [Cu<sub>2</sub>(L<sup>1</sup>)(prz)] · H<sub>2</sub>O (Mazurek et al. [8]); <sup>7</sup> [Cu<sub>2</sub>(L<sup>1</sup>)(prz)] (Nishida and Kida [7]); <sup>8</sup> [Cu<sub>2</sub>(L)(prz)] (Doman et al. [30]); <sup>9</sup> [Cu<sub>2</sub>(L)(prz)] (Gupta et al. [51]); <sup>g</sup> (Cu-O) is the average distance between the copper and the bridging O atoms; <sup>h</sup> Dihedral angle between coordination planes; <sup>i</sup> Sum of angles around the oxygen atom.

of the bonds around the bridging oxygen atom, the length of the copper-oxygen bridging bonds, and the Cu-O-Cu bridging angle. The most widely accepted factor correlating structure and magnetism is the Cu-O-Cu bridging angle [37–42]. Plots of the Cu...Cu distance, the dihedral angle ( $\phi$ ) between the two copper planes and the Cu-O-Cu bridge angle  $-2J$  versus are shown in Figure 6. It is clear that there is no simple correlation of the Cu-O-Cu bridge angle, the Cu...Cu distance and the dihedral angle ( $\phi$ ) with the strength of the exchange interaction. Thus, all the criteria so far widely accepted have failed to account for the experimental results. Accordingly, we have examined the or-

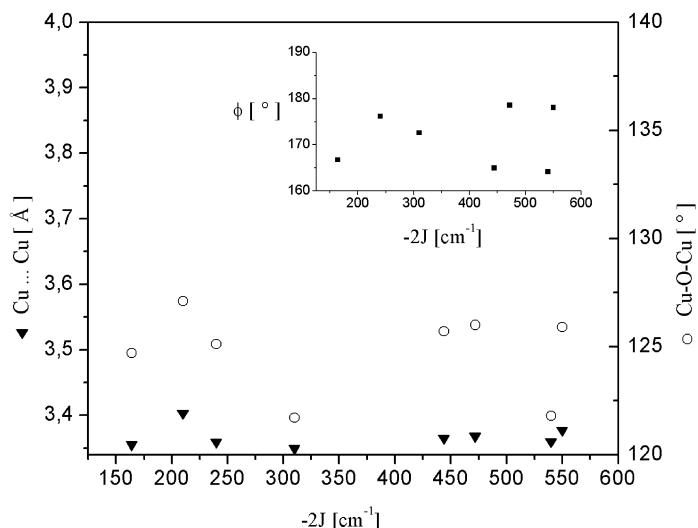


Fig. 6. Plots of the Cu...Cu distance (▲) and the Cu-O-Cu angle (○) versus the  $-2J$  value of the structurally similar complexes listed in Table 5. The inset shows a plot of the dihedral angle (■) between two copper-containing square planes versus  $-2J$ .

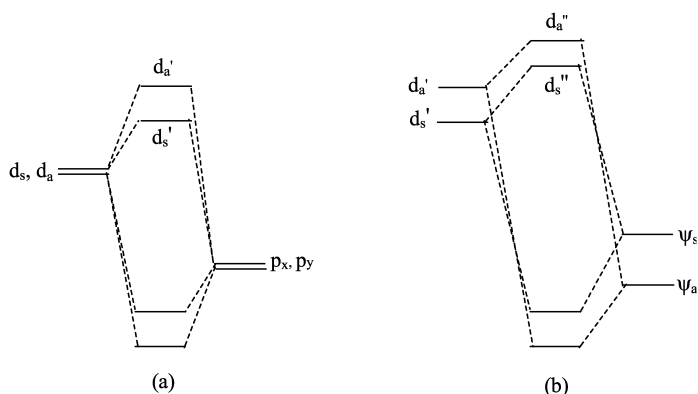


Fig. 7. The orbital energy level diagrams showing the interaction between the magnetic orbitals and bridging group orbitals, (a) for a single alkoxide- or hydroxide-bridged system; (b) for an additional bridging ligand.

bitals contributions to the superexchange interaction in more detail.

#### Orbitals Contributing to Superexchange Interaction

Based on the crystal structure of **1** and the closely the similar spectral properties of **1** and **2** [cf. the IR spectra of **1** and **2**, and the identical d-d band positions of **1** and **2**] we can assume that the present complexes have predominantly square-based copper(II) centers. The difference in magnitude of the coupling constant of the single alkoxide bridged and doubly hetero-bridged dinuclear copper complexes may be explained by the metal-ligand orbital overlap. In the single  $\mu$ -alkoxo-bridged dinuclear copper complexes, when the Cu-O-Cu angle is larger than  $90^\circ$  ( $120$ – $135.5^\circ$ ), the  $d_a$  overlap with  $p_x$  is larger than the  $d_s$  overlap with  $p_y$ . Consequently,  $d_a$  and  $d_s$  split, as illustrated in Fig-

ure 7a. Thus,  $d_a^I$  and  $d_s^I$  molecular orbitals are formed. A large energy separation of  $d_a^I$  and  $d_s^I$  leads to a strong antiferromagnetic interaction. In the presence of a second bridging ligand, either a complementary or a countercomplementary effect on the spin exchange interaction may arise due to further interactions of the symmetric ( $\psi_a$ ) and antisymmetric ( $\psi_s$ ) combinations with the  $d_a^I$  and  $d_s^I$  MO's. This interaction results in the formation of  $d_a^{II}$  and  $d_s^{II}$  (Fig. 7b).

The exchange coupling constant for the hydroxo-bridged Cu(II) complexes was evaluated by calculating the energy difference between triplet (T) and singlet (S) states (using  $\mathbf{H} = -2J\mathbf{S}_1\cdot\mathbf{S}_2$ ) [43],

$$-2j = E_T - E_S = -2K_{ab} + \frac{(\epsilon_1 - \epsilon_2)^2}{J_{aa} - J_{ab}}, \quad (2)$$

where,  $K_{ab}$ ,  $J_{aa}$ , and  $J_{ab}$  are the exchange integral and

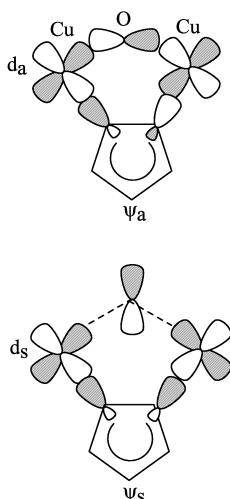


Fig. 8. Metal-3,5-dimethylpyrazolate orbital symmetry combinations.

one-center and two-center Coulomb repulsion integrals, respectively, and  $\varepsilon_1$  and  $\varepsilon_2$  are the energy levels of the HOMO and LUMO. The value of  $K_{ab}$  is always positive, so the first term in (2) contributes to the ferromagnetic interaction, while the second term, which is always positive, contributes to the antiferromagnetic interaction. The energy difference between two molecular orbitals ( $\varepsilon_1 - \varepsilon_2$ ), which corresponds to the HOMO-LUMO energy gap, determines the magnitude of the antiferromagnetic interaction. A stronger antiferromagnetic interaction is expected for the system with the larger HOMO-LUMO energy gap. The numerator of the second term “ $(\varepsilon_1 - \varepsilon_2)^2$ ” is proportional to the overlap integral between the magnetic orbitals. The overlap integrals of interacting orbitals are an important factor to increase or decrease the energy separation. If  $\psi_a$  overlaps more effectively with  $d_a$  than  $\psi_s$  with  $d_s$ , the overlap integrals of the interacting orbitals may affect the 3,5-dimethylpyrazolate bridge to act in a complementary fashion with the alkoxide bridge, and strong antiferromagnetic interactions arise (Fig. 8). Nishida *et al.* [44] show that the energies of  $d_a^{\text{II}}$  and  $d_s^{\text{II}}$  depend on two factors, (i) the energy differences between the interacting orbitals,  $E(d_a)$  and  $E(\psi_a)$ ,  $E(d_s)$  and  $E(\psi_s)$ , and (ii) the overlap integrals between the interacting orbitals,  $S(d_a, \psi_a)$  and  $S(d_s, \psi_s)$ .

First we carried out molecular orbital calculations of the 3,5-dimethylpyrazolate by ab-initio restricted Hartree-Fock (RHF) methods and investigated the interaction between the d orbitals and the HOMO's of the 3,5-dimethylpyrazolate in order to clarify the in-

fluence of the second bridging ligand on the superexchange interaction. We determined approximate values for the overlap integrals between the interaction orbital,  $S(d_a, \psi_a)$  and  $S(d_s, \psi_s)$  and calculated the difference between  $S(d_a, \psi_a)$  and  $S(d_s, \psi_s)$  for the compound **1**. The rigorous definition and the process of the calculation are given in the Appendix. In a preceding study, we have also determined these values for compounds **3**, **4**, and **5** [9, 10, 11]. We have found the following results from our calculations:

$$S(a-s)(\mathbf{5}) > S(a-s)(\mathbf{3}) > S(a-s)(\mathbf{1}) > S(a-s)(\mathbf{4}).$$

There is a similar relation between the strength of the superexchange interaction of the complexes:

$$2J(\mathbf{5}) > 2J(\mathbf{3}) > 2J(\mathbf{1}) > 2J(\mathbf{4}).$$

This clearly indicates that the difference in the magnitude of the coupling constants is explained by overlap integrals between the interaction orbital.

#### Extended Hückel Molecular Orbital (EHMO) Calculations

In addition to the above calculations, we have also carried out Extended Hückel Molecular Orbital (EHMO) calculations. EHMO calculations have been performed in order to gain insight into the molecular orbitals that participate in the superexchange pathway. Using the crystallographic coordinates for compound **1**, an energy difference of 1.11 eV is obtained between the HUMO and LUMO. The calculations indicate the following orbital participations: Cu d orbitals, 25%; N p orbitals, 64%; O p orbitals, 8% for LUMO and Cu d orbitals, 70%; N p orbitals, 13%; O p orbitals, 10% for HOMO.

A graph of HOMO and LUMO orbitals for the compound **1** is depicted in Figure 9. As can be observed,

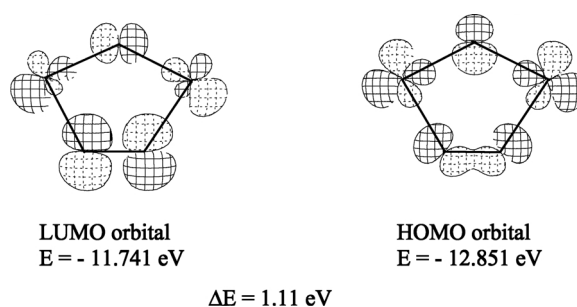


Fig. 9. Drawing of HOMO and LUMO frontier orbitals (for orbitals contributing more than 1%) obtained for compound **1**.

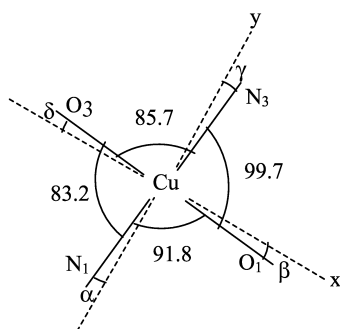


Fig. 10. Projection of Cu1 and the donor atoms in the best plane formed by these atoms. (The broken lines are the axes of the d orbitals).

the Cu metal centers use  $d_{x^2-y^2}$  type orbitals for a  $\sigma^*$  interaction with  $P_N$  and  $P_O$  orbitals. The LUMO orbital is a symmetric  $d_{Cu}-d_{Cu}$  orbital combination, whereas the HOMO orbital is a  $d_{Cu}-d_{Cu}$  antisymmetric combination.

### Supplementary Data

Crystallographic data (atomic coordinates, atomic displacement parameters and bond geometries) for the structure reported in the paper have been deposited in the Cambridge Crystallographic Data Center (CCDC) as supplementary material with the deposition number CCDC-200445. E-mail: deposit@ccdc.cam.ac.

### Acknowledgements

This work was supported by the Research Funds of the University of Ankara (98-05-05-02) and the University of Balıkesir (99/3). Hulya KARA thanks the Munir Bırsel Found-TUBITAK for financial support. Y. Elerman and A. Elmali want to thank for an Alexander von Humboldt Fellowship.

### Appendix

#### Determination of the Orientation of the Magnetic d Orbitals

Figure 10 shows the projection of Cu1 and the donor atoms onto the coordination plane, together with the axes of the magnetic d orbitals (broken lines). The angles formed by the coordinative bonds and the axes of the d orbitals are denoted as  $\alpha$ ,  $\beta$ ,  $\gamma$ , and  $\delta$ . In order to fulfill the requirement of maximum overlap, the fol-

lowing function was minimised:

$$\begin{aligned} F(\alpha) &= \alpha^2 + \beta^2 + \gamma^2 + \delta^2 \\ &= \alpha^2 + (\alpha + 90 - 91.8)^2 \\ &\quad + (\alpha + 180 - 91.8 - 99.7)^2 \\ &\quad + (\alpha + 270 - 91.8 - 99.7 - 85.7)^2 \\ &= 4\alpha^2 - 41\alpha + 187.33. \end{aligned} \quad (1)$$

If  $dF(\alpha)/d\alpha = 0$ , then  $\alpha = 5.125^\circ$ . The same value was obtained for  $\alpha$  about the coordination plane of Cu2.

#### Determination of overlap integrals between $d_s$ and $\psi_s$ and between $d_a$ and $\psi_a$ :

When the  $x$  and  $y$  axes in Fig. 10 are rotated by  $\alpha$ , the  $d_1$  orbital is expressed in terms of the new coordinate system as

$$d_1 = (\cos(2\alpha))d_{x^2-y^2} + (\sin(2\alpha))d_{xy}. \quad (2)$$

The  $\psi_s$  and  $\psi_a$  orbitals of the 3,5- dimethylpyrazolate ion can be expressed as the sum of the orbitals on N1 and N2 and the neighbouring carbon atoms

$$\psi_s = \phi_{s1} + \phi_{s2} + \phi_{sC}, \quad (3)$$

$$\psi_a = \phi_{a1} + \phi_{a2} + \phi_{aC}. \quad (4)$$

These orbitals can be expressed in terms of the new coordinate system in which the  $y$ -axis is on the Cu1-N1 bond.

$$\begin{aligned} \phi_{s1} &= 0.14556s + 0.21598((\cos 30^\circ)p_x + (\sin 30^\circ)p_y) \\ &\quad + 0.02367(-(\cos 60^\circ)p_x + (\sin 60^\circ)p_y), \end{aligned} \quad (5)$$

$$\phi_{s1} = 0.14556s + 0.17521p_x + 0.12799p_y.$$

From (2) and (5)

$$\begin{aligned} S(d_1, \phi_{s1}) &= 0.14556(\cos(2\alpha))S(3d, 2s) \\ &\quad + 0.12799(\cos(2\alpha))S(3d_\sigma, 2p_\sigma) \\ &\quad + 0.17521(\sin(2\alpha))S(3d_\pi, 2p_\pi). \end{aligned}$$

Since  $d_s = (d_1 - d_2) / 2^{1/2}$  and  $S(d_2, \phi_{s2}) = -S(d_1, \phi_{s1})$ ,

$$\begin{aligned} S(d_s, \psi_s) &= 2S(d_1, \phi_{s1})/2^{1/2}, \\ S(d_s, \Psi_s) &= 0.2058(\cos(2\alpha))S(3d, 2s) \\ &\quad + 0.1810(\cos(2\alpha))S(3d_\sigma, 2p_\sigma) \\ &\quad + 0.2477(\sin(2\alpha))S(3d_\pi, 2p_\pi). \end{aligned} \quad (6)$$



In a similar way,  $S(d_a, \psi_a)$  was obtained as follows:

$$\begin{aligned} S(d_a, \Psi_a) = & 0.0001(\cos(2\alpha))S(3d, 2s) \\ & + 0.4761(\cos(2\alpha))S(3d_\sigma, 2p_\sigma) \\ & - 0.2749(\sin(2\alpha))S(3d_\pi, 2p_\pi). \end{aligned} \quad (7)$$

From (6) and (7) for compound **1**

$$\begin{aligned} S(a-s) = & S(d_a, \Psi_a) - S(d_s, \Psi_s) \\ = & -0.20585(\cos(2\alpha))S(3d, 2s) \\ & + 0.2951(\cos(2\alpha))S(3d_\sigma, 2p_\sigma) \\ & - 0.5226(\sin(2\alpha))S(3d_\pi, 2p_\pi). \end{aligned} \quad (8)$$

Rough values of the overlap integrals for the present complexes can be estimated from the tables of Jaffe *et al.* [45] and Kuruda and Ito [46];  $S(3d, 2s) \approx 0.04$ ,  $S(3d_\sigma, 2p_\sigma) \approx 0.06$ ,  $S(3d_\pi, 2p_\pi) \approx 0.02$ . Comparing

these values with (8), one can conclude that  $S(a-s)$  is definitely larger than zero in the case of **1**.

In the case of **1**,  $\alpha = 5.125^\circ$ ; hence

$$S(a-s) = 0.00747. \quad (9)$$

For **3**, **4**, and **5**, overlap integrals are also obtained by the same principle [11, 12]: In case of **3**,  $\alpha = 6.125^\circ$ ; hence

$$S(a-s) = 0.01074. \quad (10)$$

In case of **4**,  $\alpha = 6.46^\circ$ ; hence

$$S(a-s) = 0.00419. \quad (11)$$

In case of **5**,  $\alpha = 5.465^\circ$ ; hence

$$S(a-s) = 0.01296. \quad (12)$$

- [1] O. Kahn, Y. Pei, and Y. Journaux, In *Inorganic Materials*; Q. W. Bruce and D. O'Hare, Eds.; John Wiley and Sons; Chichester, U.K. 1992.
- [2] O. Kahn, *Molecular Magnetism*; VCH publishers: New York 1993.
- [3] D. Gatteschi, O. Kahn, J.S. Miller, and F. Palacio, *Magnetic Molecular Materials*, Kluwer Academic; Dordrecht, The Netherlands 1991.
- [4] V. V. Volkov, Y. V. Rakitin, and V. T. Kalinnikov, *Koord. Khim.* **9**, 31 (1983).
- [5] V. H. Crawford, H. W. Richardson, J. R. Wasson, D. J. Hodgson, and W. E. Hatfield, *Inorg. Chem.* **15**, 2107 (1976).
- [6] A. Bencini and D. Gatteschi, *Inorg. Chim. Acta* **31**, 11 (1978).
- [7] H. Astheimer and W. Haase, *J. Chem. Phys.* **85**, 1427 (1986).
- [8] C. Blanchet-Boiteux and J.-M. Mouesca, *J. Phys. Chem. A* **104**, 2091 (2000).
- [9] H. Kara, Y. Elerman, and K. Prout, *Z. Naturforsch.* **55b**, 796 (2000).
- [10] H. Kara, Y. Elerman, and K. Prout, *Z. Naturforsch.* **56b**, 719 (2001).
- [11] Y. Elerman, H. Kara, and A. Elmali, *Z. Naturforsch.* **56b**, 1129 (2001).
- [12] L. Merz and W. J. Haase, *Chem. Soc. Dalton Trans.* 1980, p. 875.
- [13] S. J. Swithenby, *Contemp. Phys.* **15**, 249 (1974).
- [14] Al. Weiss and H. Witte, *Magnetochemie*, Verlag Chemie, Weinheim 1973.
- [15] Enraf-Nonius DIP2000 diffractometer control software, DENZO, Otwinowski, Z. & Minor, W. (1996), *Processing of X-ray Diffraction Data Collected in Oscillation Mode. Methods Enzymol.* **276**, 307 (1997). Ed Carter, C. W. & Sweet, R. M., Academic Press, New York.
- [16] DIFABS, N. Walker, and D. Stuart, *Acta Cryst.* **A39**, 158 (1983).
- [17] A. Altomare, G. Cascarano, G. Giacovazzo, A. Guagliardi, M. C. Burla, G. Polidori, and M. Camalli, SIR92 – a program for automatic solution of crystal structures by direct methods. *J. Appl. Cryst.* **27**, 435 (1994).
- [18] CRYSTALS, D. J. Watkin, C. K. Prout, J. R. Caruthers, and P. W. Betteridge, CRYSTALS, Issue 10. Chemical Crystallography Laboratory, OXFORD, UK 1996.
- [19] L. J. Farrugia, *J. Appl. Cryst.* **30**, 565 (1997).
- [20] Gaussian 98, Revision A. 3, M. J. Frisch, G. W. Trucks, H. B. Schlegel, G. E. Scuseria, M. A. Robb, J. R. Cheeseman, V. G. Zakrzewski, J. A. Montgomery, R. E. Stratmann, J. C. Burant, S. Dapprich, J. M. Millam, A. D. Daniels, K. N. Kudin, M. C. Strain, O. Farkas, J. Tomasi, V. Barone, M. Cossi, R. Cammi, B. Menucci, C. Pomelli, C. Adamo, S. Clifford, J. Ochterski, G. A. Petersson, P. Y. Ayala, Q. Cui, K. Morokuma, D. K. Malick, A. D. Rabuck, K. Raghavachari, J. B. Foresman, J. Cioslowski, J. V. Ortiz, B. B. Stefanov, G. Liu, A. Liashenko, P. Piskorz, I. Komaromi, R. Gomberts, R. L. Martin, D. J. Fox, T. Keith, M. A.

- Al-Laham, C. Y. Peng, A. Nanayakkara, C. Gonzalez, M. Challacombe, P. M. W. Gill, B. Jhonson, W. Chen, M. W. Wong, J. L. Andres, M. Head-Gordon, E. S. Replogle, and J. A. Pople, Gaussian, Inc., Pittsburgh PA, 1998.
- [21] W. J. Hehre, R. F. Stewart, and J. A. Pople, *J. Chem. Phys.* **51**, 2657 (1969).
- [22] R. Hoffmann, *J. Chem. Phys.* **39**, 1397 (1963).
- [23] R. Hoffmann and W. N. Lipscomb, *J. Chem. Phys.* **36**, 2179 (1962).
- [24] C. Mealli and D. M. Proserpio, Computer Aided Composition of Atomic Orbitals, (CACAO program) PC version, July 1992. See also: *J. Chem. Educ.* **67**, 3399 (1990).
- [25] B. C. Whitmore and R. Eisenberg, *Inorg. Chem.* **1**, 22 (1983).
- [26] W. M. Coleman and L. Taylor, *Inorg. Chem.* **10**, 2195 (1971).
- [27] Y. Nakao, M. Yamashita, T. Itoh, W. Mori, S. Susuki, and T. Sakurai, *Bull. Chem. Soc. Jpn.* **67**, 260 (1994).
- [28] G. A. Van Albada, W. J. J. Smeets, A. L. Spek, and J. Redijk, *Inorg. Chem. Acta* **260**, 151 (1997).
- [29] G. A. Van Albada, M. T. Lakin, N. Veldman, A. L. Spek, and J. Redijk, *Inorg. Chem.* **34**, 4910 (1995).
- [30] D. Black, A. J. Blake, K. P. Dancey, A. Harrison, M. McPartlin, S. Parsons, P. A. Tasker, G. Whittaker, and M. Schrder, *J. Chem. Soc. Dalton Trans.* 1998, p. 3953.
- [31] A. Asokan, B. Varghese, and P. T. Manoharan, *Inorg. Chem.* **38**, 4393 (1999).
- [32] O. Castillo, I. Muga, A. Luque, J. M. Gutie'rrez-Zorrilla, J. Sertucha, P. Vitoria, and P. Roma'n, *Polyhedron* **18**, 1235 (1999).
- [33] L. K. Thompson, S. K. Mandal, S. S. Tandon, J. N. Bridson, and M. K. Park, *Inorg. Chem.* **35**, 3117 (1996).
- [34] C. Li, N. Kanehisa, Y. Miyagi, Y. Nakao, S. Takamizawa, W. Mori, and Y. Kai, *Bull. Chem. Soc. Jpn.* **70**, 2429 (1997).
- [35] T. N. Doman, D. E. Williams, J. F. Banks, R. M. Buchanan, H. R. Chang, R. J. Webb, and D. N. Hendrickson, *Inorg. Chem.* **29**, 1058 (1990).
- [36] C. J. O'Connor, *Prog. Inorg. Chem.* **29**, 203 (1982).
- [37] D. M. Duggan and N. Hendrickson, *Inorg. Chem.* **12**, 2422 (1973).
- [38] R. E. Coffmann and G. R. Buettner, *J. Phys. Chem.* **83**, 2387 (1979).
- [39] M. Gerloch and J. H. Hardring, *Proc. Roy. Soc. London* **A360**, 211 (1978).
- [40] T. R. Felthouse, E. J. Laskowski, and D. H. Hendrickson, *Inorg. Chem.* **16**, 1077 (1977).
- [41] D. N. Hendrickson, In *Magneto-Structural Correlations in Exchange-Coupled Systems*: R. Willet, D. Gatteschi, and O. Kahn, Reidel, Dordrecht, The Netherlands, 1984.
- [42] O. Kahn and B. Briat, *J. Chem. Soc. Faraday Trans.* 1976, p. 268.
- [43] P. J. Hay, J. C. Thibeault, and R. Hoffmann, *J. Amer. Chem. Soc.* **97**, 4887 (1975).
- [44] Y. Nishida and S. Kida, *Inorg. Chem.* **27**, 447 (1988).
- [45] (a) H. H. Jaffe and G. O. Doal, *J. Chem. Phys.* **21**, 196 (1953). (b) H. H. Jaffe, *Ibid.* **21**, 258 (1953).
- [46] Y. Kuroda and K. Ito, *Nippon Kagaku Zasshi* **76**, 545 (1955).